Eur. Phys. J. B **15**, 607–614 (2000)

THE EUROPEAN PHYSICAL JOURNAL B

EDP Sciences

Pseudogap effects on the c-axis charge dynamics in copper oxide materials

Shiping Feng[1,2,3,a], Feng Yuan[2], and Weiqiang Yu[2]

[1] CCAST (World Laboratory) PO Box 8730, Beijing 100080, P.R. China
[2] Department of Physics, Beijing Normal University, Beijing 100875, P.R. China
[3] National Laboratory of Superconductivity, Academia Sinica, Beijing 100080, P.R. China

Received 29 July 1999 and Received in final form 24 January 2000

Abstract. The c-axis charge dynamics of copper oxide materials in the underdoped and optimally doped regimes has been studied by considering the incoherent interlayer hopping. It is shown that the c-axis charge dynamics for the chain copper oxide materials is mainly governed by the scattering from the in-plane fluctuation, and the c-axis charge dynamics for the no-chain copper oxide materials is dominated by the scattering from the in-plane fluctuation incorporating with the interlayer disorder, which would be suppressed when the holon pseudogap opens at low temperatures and lower doping levels, leading to the crossovers to the semiconducting-like range in the c-axis resistivity and the temperature linear to the nonlinear range in the in-plane resistivity.

PACS. 71.27.+a Strongly correlated electron systems; heavy fermions – 72.10.-d Theory of electronic transport; scattering mechanisms – 74.72.-h High-T_c compounds

1 Introduction

It has become clear in the past several years that copper oxide materials are among the most complex systems studied in condensed matter physics, and show many unusual normal-state properties. The complications arise mainly from (1) strong anisotropy in the properties parallel and perpendicular to the CuO_2 planes which are the key structural element in the whole copper oxide superconducting materials, and (2) extreme sensitivity of the properties to the compositions (stoichiometry) which control the carrier density in the CuO_2 plane [1], while the unusual normal-state feature is then closely related to the fact that these copper oxide materials are doped Mott insulators, obtained by chemically adding charge carriers to a strongly correlated antiferromagnetic (AF) insulating state, therefore the physical properties of these systems mainly depend on the extent of dopings, and the regimes have been classified into the underdoped, optimally doped, and overdoped, respectively [2]. The normal-state properties of copper oxide materials in the underdoped and optimally doped regimes exhibit a number of anomalous properties in the sense that they do not fit in the conventional Fermi-liquid theory [2,3], and the mechanism for the superconductivity in copper oxide materials has been widely recognized to be closely associated with the anisotropic normal-state properties [4,5]. Among the striking features of the normal-state properties in the underdoped and optimally doped regimes, the physical quantity which most evidently displays the anisotropic property in copper oxide materials is the charge dynamics [5], which is manifested by the optical conductivity and resistivity. It has been show from the experiments that the in-plane charge dynamics is rather universal within the whole copper oxide materials [2,5]. The in-plane optical conductivity for the same doping is nearly materials independent both in the magnitude and energy dependence, and shows the non-Drude behavior at low energies and anomalous midinfrared band in the charge-transfer gap, while the in-plane resistivity $\rho_{ab}(T)$ exhibits a linear behavior in the temperature in the optimally doped regime and a nearly temperature linear dependence with deviations at low temperatures in the underdoped regime [2,5]. By contrast, the magnitude of the c-axis charge dynamics in the underdoped and optimally doped regimes is strongly materials dependent, *i.e.*, it is dependent on the species of the building blocks in between the CuO_2 planes [6–10]. In the underdoped and optimally doped regimes, the experimental results [6–10] show that the ratio $R = \rho_c(T)/\rho_{ab}(T)$ ranges from $R \sim 100$ to $R > 10^5$, this large magnitude of the resistivity anisotropy reflects that the c-axis mean free path is shorter than the interlayer distance, and the carriers are tightly confined to the CuO_2 planes, and also is the evidence of the incoherent charge dynamics in the c-axis direction. For the copper oxide materials without the Cu-O chains in between the CuO_2 planes [9], such as $La_{2-x}Sr_xCuO_4$ systems, the transferred weight in the c-axis conductivity

[a] e-mail: spfeng@sun.ihep.ac.cn

forms a band peaked at high energy $\omega \sim 2$ eV, and the low-energy spectral weight is quite small and spread over a wide energy range instead of forming a peak at low energies, in this case the behavior of the c-axis temperature dependent resistivity $\rho_c(T)$ is characterized by a crossover from the high temperature metallic-like to the low temperature semiconducting-like [9]. However, for these copper oxide materials with the Cu-O chains in between the CuO_2 planes [10], such as $YBa_2Cu_3O_7$ systems, the c-axis conductivity exhibits the non-Drude behavior at low energies and weak midinfrared band, moreover, this weak midinfrared band rapidly decrease with reducing dopings or increasing temperatures, while the c-axis resistivity $\rho_c(T)$ is linear in temperatures in the optimally doped regime, and shows a crossover from the high temperature metallic-like behavior to the low temperature semiconducting-like behavior in the underdoped regime [10]. Therefore there are some subtle differences between the chain and no-chain copper oxide materials.

The c-axis charge dynamics of copper oxide materials has been addressed from several theoretical viewpoints [11–15]. Based on the concept of dynamical dephasing, Leggett [11] thus proposed that the c-axis conduction has to do with scatterings from in-plane thermal fluctuations, and depends on the ratio of the interlayer hopping rate of CuO_2 sheets to the thermal energy. While the theory of tunneling c-axis conductivity in the incoherent regime has been given by many researchers [12]. Based on a highly anisotropic Fermi-liquid, some effect from the interlayer static disorder or dynamical one has been discussed [13]. The similar incoherent conductivity in the coupled fermion chains has been in more detail studied by many authors within the framework of the non-Fermi-liquid theory [14]. Moreover, the most reliable result for the c-axis charge dynamics from the model relevant to copper oxide materials has been obtained by the numerical simulation [15]. It has been argued that the in-plane resistivity deviates from the temperature linear behavior and temperature coefficient of the c-axis resistivity change sign, showing semiconducting-like behavior at low temperatures are associated with the effect of the pseudogap [9,10]. To shed light on this issue, we, in this paper, apply the fermion-spin approach [16,17] to study the c-axis charge dynamics by considering the interlayer coupling.

The paper is organized as follows. The theoretical framework is presented in Section 2. In the case of the incoherent interlayer hopping, the c-axis current-current correlation function (then the c-axis optical conductivity) is calculated in terms of the in-plane single-particle spectral function by using standard formalisms for the tunneling in metal-insulator-metal junctions [18,19]. Within this theoretical framework, we discuss the c-axis charge dynamics of the chain copper oxide materials in Section 3. It is shown that the c-axis charge dynamics of the chain copper oxide materials is mainly governed by the scattering from in-plane charged holons due to spinon fluctuations, and the behavior of the c-axis resistivity is the metallic-like in the optimally doped regime and the semiconducting-like in the underdoped regime at low temperatures. In Section 4, the c-axis charge dynamics of the no-chain copper oxide materials is discussed. Our result shows that the scattering from the in-plane fluctuation incorporating with the interlayer disorder dominates the c-axis charge dynamics for the no-chain copper oxide materials. In this case, the c-axis resistivity exhibits the semiconducting-like behavior in the underdoped and optimally doped regimes at low temperatures. Section 5 is devoted to a summary and discussions. Our results also show that the crossover to the semiconducting-like range in $\rho_c(T)$ is obviously linked with the crossover from the temperature linear to the nonlinear range in $\rho_{ab}(T)$, and the common origin for these crossovers is due to the existence of the holon pseudogap at low temperatures and lower doping levels.

2 Theoretical framework

Among the microscopic models the most simplest for the discussion of doped Mott insulators is the t-J model [20], which is originally introduced as an effective Hamiltonian of the Hubbard model in the strong coupling regime, where the electron become strongly correlated to avoid the double occupancy. The interest in the t-J model is stimulated by many researchers' suggestions that it may contain the essential physics of copper oxide materials [20,21]. On the other hand, there is a lot of evidence from the experiments and numerical simulations in favour of the t-J model as the basic underlying microscopic model [3,22]. Within each CuO_2 plane, the physics property may be described by the two-dimensional (2D) t-J model,

$$H_l = -t\sum_{i\hat{\eta}\sigma} C^{\dagger}_{li\sigma}C_{li+\hat{\eta}\sigma} + \text{h.c.} - \mu\sum_{i\sigma} C^{\dagger}_{li\sigma}C_{li\sigma} + J\sum_{i\hat{\eta}} \mathbf{S}_{li}\cdot\mathbf{S}_{li+\hat{\eta}}, \quad (1)$$

supplemented by the on-site local constraint $\sum_\sigma C^{\dagger}_{li\sigma}C_{li\sigma} \leq 1$ to avoid the double occupancy, where $\hat{\eta} = \pm a_0\hat{x}, \pm a_0\hat{y}$, a_0 is the lattice constant of the square planar lattice, which is set as the unit hereafter, i refers to planar sites within the lth CuO_2 plane, $C^{\dagger}_{li\sigma}$ ($C_{li\sigma}$) are the electron creation (annihilation) operators, $\mathbf{S}_{li} = C^{\dagger}_{li}\sigma C_{li}/2$ are the spin operators with $\sigma = (\sigma_x, \sigma_y, \sigma_z)$ as the Pauli matrices, and μ is the chemical potential. Then the hopping between CuO_2 planes is considered as [15]

$$H = -t_c\sum_{l\hat{\eta}_c i\sigma} C^{\dagger}_{li\sigma}C_{l+\hat{\eta}_c i\sigma} + \text{h.c.} + \sum_l H_l, \quad (2)$$

where $\hat{\eta}_c = \pm c_0\hat{z}$, c_0 is the interlayer distance, and has been determined from the experiments [23] as $c_0 > 2a_0$. As mentioned above, the experimental results show that the c-axis charge dynamics in the underdoped and optimally doped regimes is incoherent, therefore the c-axis momentum can not be defined [24]. Moreover, the absence

of the coherent *c*-axis charge dynamics is a consequence of the weak interlayer hopping matrix element t_c, but also of a strong intralayer scattering, *i.e.*, $t_c \ll t$, and therefore the common CuO_2 planes in copper oxide materials clearly dominate the most normal-state properties. In this case, the most relevant for the study of the *c*-axis charge dynamics is the results on the in-plane conductivity $\sigma_{ab}(\omega)$ and related single-particle spectral function $A(k,\omega)$.

Since the strong electron correlation in the t-J model manifests itself by the electron single occupancy on-site local constraint, then the crucial requirement is to impose this electron on-site local constraint for a proper understanding of the physics of copper oxide materials. To incorporate this local constraint, the fermion-spin theory based on the charge-spin separation has been proposed [16,17]. According to the fermion-spin theory, the constrained electron operators in the t-J model is decomposed as [16],

$$C_{li\uparrow} = h^{\dagger}_{li} S^{-}_{li}, \qquad C_{li\downarrow} = h^{\dagger}_{li} S^{+}_{li}, \tag{3}$$

with the spinless fermion operator h_i keeps track of the charge (holon), while the pseudospin operator S_i keeps track of the spin (spinon). The main advantage of this approach is that the electron on-site local constraint can be treated exactly in analytical calculations. In this case, the low-energy behavior of the t-J model (2) in the fermion-spin representation can be written as [25],

$$H = t_c \sum_{l\hat{\eta}_c i} h^{\dagger}_{l+\hat{\eta}_c i} h_{li} (S^{+}_{li} S^{-}_{l+\hat{\eta}_c i} + S^{-}_{li} S^{+}_{l+\hat{\eta}_c i}) + \sum_{l} H_l, \tag{4a}$$

$$H_l = t \sum_{i\hat{\eta}} h^{\dagger}_{li+\hat{\eta}} h_{li} (S^{+}_{li} S^{-}_{li+\hat{\eta}} + S^{-}_{li} S^{+}_{li+\hat{\eta}}) + \mu \sum_{i} h^{\dagger}_{li} h_{li} + J_{\rm eff} \sum_{i\hat{\eta}} (\mathbf{S}_{li} \cdot \mathbf{S}_{li+\hat{\eta}}), \tag{4b}$$

where $J_{\rm eff} = J[(1-\delta)^2 - \phi^2]$, the in-plane holon particle-hole parameter $\phi = \langle h^{\dagger}_{li} h_{li+\hat{\eta}} \rangle$, and S^{+}_{li} and S^{-}_{li} are the pseudospin raising and lowering operators, respectively. As a consequence, the kinetic part in the t-J model has been expressed as the holon-spinon interaction in the fermion-spin representation, which dominates the charge and spin dynamics in copper oxide materials in the underdoped and optimally doped regimes. The spinon and holon may be separated at the mean-field level, but they are strongly coupled beyond mean-field approximation (MFA) due to fluctuations.

The mean-field theory within the fermion-spin formalism in the underdoped and optimally doped regimes without AF long-range-order (AFLRO) has been developed [17], and the in-plane mean-field spinon and holon Green's functions $D^{(0)}_{ab}(i-j,\tau-\tau') = -\langle T_\tau S^{+}_{li}(\tau) S^{-}_{lj}(\tau') \rangle_0$ and $g^{(0)}_{ab}(i-j,\tau-\tau') = -\langle T_\tau h_{li}(\tau) h^{\dagger}_{lj}(\tau') \rangle_0$ have been evaluated [17] as,

$$D^{(0)}_{ab}(\mathbf{k},\omega) = \frac{B_k}{2\omega(k)} \left(\frac{1}{\omega - \omega(k)} - \frac{1}{\omega + \omega(k)} \right), \tag{5}$$

$$g^{(0)}_{ab}(\mathbf{k},\omega) = \frac{1}{\omega - \xi_k}, \tag{6}$$

respectively, where $B_k = \lambda[(2\epsilon\chi_z + \chi)\gamma_k - (\epsilon\chi + 2\chi_z)]$, $\gamma_{\mathbf{k}} = (1/Z)\sum_{\eta} e^{i\mathbf{k}\cdot\hat{\boldsymbol{\eta}}}$, $\lambda = 2ZJ_{\rm eff}$, $\epsilon = 1 + 2t\phi/J_{\rm eff}$, Z is the number of the nearest neighbor sites at the plane, while the in-plane mean-field spinon spectrum

$$\begin{aligned}\omega^2(k) = {} & \lambda^2 \left(\alpha\epsilon[\chi_z\gamma_k + \frac{1}{2Z}\chi] - [\alpha C_z + \frac{1}{4Z}(1-\alpha)] \right) \\ & \times (\epsilon\gamma_k - 1) \\ & + \lambda^2 \left(\alpha\epsilon[\frac{1}{2}\chi\gamma_k + \frac{1}{Z}\chi_z] - \frac{1}{2}\epsilon[\alpha C + \frac{1}{2Z}(1-\alpha)] \right) \\ & \times (\gamma_k - \epsilon),\end{aligned} \tag{7}$$

and the in-plane mean-field holon spectrum $\xi_k = 2Z\chi t\gamma_k + \mu$, with the in-plane spinon correlation functions $\chi = \langle S^{+}_{li} S^{-}_{li+\hat{\eta}} \rangle$, $\chi_z = \langle S^{z}_{li} S^{z}_{li+\hat{\eta}} \rangle$, $C = (1/Z^2)\sum_{\hat{\eta},\hat{\eta}'} \langle S^{+}_{li+\hat{\eta}} S^{-}_{li+\hat{\eta}'} \rangle$, and $C_z = (1/Z^2) \times \sum_{\hat{\eta},\hat{\eta}'} \langle S^{z}_{li+\hat{\eta}} S^{z}_{li+\hat{\eta}'} \rangle$. In order not to violate the sum rule of the correlation function $\langle S^{+}_{li} S^{-}_{li} \rangle = 1/2$ in the case without AFLRO, the important decoupling parameter α has been introduced in the mean-field calculation [17], which can be regarded as the vertex correction. The mean-field order parameter χ, C, χ_z, C_z, ϕ, the decoupling parameter α, and chemical potential μ have been determined [17,27] by the self-consistent equations, and the results for the order parameters χ, C, χ_z, C_z, and ϕ are very close to our previous works [16] based on the 2D Jordan-Wigner approach [26]. These order parameters are doping and temperature dependence, and the detailed discussions have been given in reference [27].

Within the 2D t-J model, the in-plane charge dynamics in copper oxide materials has been discussed [25] by considering fluctuations around this mean-field solution, and the result exhibits a behavior similar to that seen in the experiments [2,3] and numerical simulations [28]. In the framework of the charge-spin separation, an electron is represented by the product of a holon and a spinon, then the external field can only be coupled to one of them. According to the Ioffe-Larkin combination rule [29,30], the physical *c*-axis conductivity $\sigma_c(\omega)$ is given by,

$$\sigma^{-1}_{c}(\omega) = \sigma^{({\rm h})-1}_{c}(\omega) + \sigma^{({\rm s})-1}_{c}(\omega), \tag{8}$$

where $\sigma^{({\rm h})}_{c}(\omega)$ and $\sigma^{({\rm s})}_{c}(\omega)$ are the contributions to the *c*-axis conductivity from holons and spinons, respectively, and can be expressed [18] as,

$$\begin{aligned}\sigma^{({\rm h})}_{c}(\omega) &= -\frac{{\rm Im}\Pi^{({\rm h})}_{c}(\omega)}{\omega}, \\ \sigma^{({\rm s})}_{c}(\omega) &= -\frac{{\rm Im}\Pi^{({\rm s})}_{c}(\omega)}{\omega},\end{aligned} \tag{9}$$

with $\Pi^{({\rm h})}_{c}(\omega)$ and $\Pi^{({\rm s})}_{c}(\omega)$ are the spinon and holon *c*-axis current-current correlation functions, respectively, which are defined as,

$$\begin{aligned}\Pi^{({\rm s})}_{c}(\tau-\tau') &= -\langle T_\tau j^{({\rm s})}_{c}(\tau) j^{({\rm s})}_{c}(\tau') \rangle, \\ \Pi^{({\rm h})}_{c}(\tau-\tau') &= -\langle T_\tau j^{({\rm h})}_{c}(\tau) j^{({\rm h})}_{c}(\tau') \rangle.\end{aligned} \tag{10}$$

Within the Hamiltonian (4), the c-axis current densities of spinons and holons are obtained by the time derivation of the polarization operator using Heisenberg's equation of motion as, $j_c^{(\mathrm{s})} = t_c e\phi_c \sum_{l\hat{\eta}_c i} \hat{\eta}_c (S_{li}^{+} S_{l+\hat{\eta}_c i}^{-} + S_{li}^{-} S_{l+\hat{\eta}_c i}^{+})$ and $j_c^{(\mathrm{h})} = 2\tilde{t}_c e\chi \sum_{l\hat{\eta}_c i} \hat{\eta}_c h_{l+\hat{\eta}_c i}^{\dagger} h_{li}$, respectively, with $\tilde{t}_c = t_c\chi_c/\chi$ is the effective interlayer holon hopping matrix element, and the order parameters χ_c and ϕ_c are defined [17] as $\chi_c = \langle S_{li}^{+} S_{l+\hat{\eta}_c i}^{-}\rangle$, and $\phi_c = \langle h_{li}^{\dagger} h_{l+\hat{\eta}_c i}\rangle$, respectively. With the help of the spinon and holon c-axis current densities, the c-axis spinon and holon current-current correlation functions (10) can be expressed as,

$$\begin{aligned}\Pi_c^{(\mathrm{s})}(\tau-\tau') &= -(t_c e\phi_c)^2 \sum_{l\hat{\eta}_c i l'\hat{\eta}_c' i'} \hat{\eta}_c\hat{\eta}_c' \langle T_\tau [S_{li}^{+}(\tau) S_{l+\hat{\eta}_c i}^{-}(\tau) \\ &+ S_{li}^{-}(\tau) S_{l+\hat{\eta}_c i}^{+}(\tau)] \\ &\times [S_{l'i'}^{+}(\tau') S_{l'+\hat{\eta}_c' i'}^{-}(\tau') + S_{l'i'}^{-}(\tau') S_{l'+\hat{\eta}_c' i'}^{+}(\tau')]\rangle, \quad (11a)\\ \Pi_c^{(\mathrm{h})}(\tau-\tau') &= -(2\tilde{t}_c e\chi)^2 \\ &\times \sum_{l\hat{\eta}_c i l'\hat{\eta}_c' i'} \hat{\eta}_c\hat{\eta}_c' \langle T_\tau h_{l+\hat{\eta}_c i}^{\dagger}(\tau) h_{li}(\tau) h_{l'+\hat{\eta}_c' i'}^{\dagger}(\tau') h_{l'i'}(\tau')\rangle, \end{aligned} \quad (11b)$$

respectively. Since the spinon operators obey the Pauli algebra, we can map the spinon operators into the spinless-fermion representation in terms of the 2D Jordan-Wigner transformation [26] or the CP^1 fermion representation for the formal many particle calculation [31]. On the other hand, in the case of the incoherent charge dynamics in the c-axis direction, *i.e.*, the independent electron propagation in the each layer, the c-axis spinon and holon current-current correlation functions are then proportional to the tunneling rate between just two adjacent planes, and can be calculated in terms of the in-plane spinon and holon Green's function $D_{ab}(k,\omega)$ and $g_{ab}(k,\omega)$, respectively, by using standard formalisms for the tunneling in metal-insulator-metal junctions [15,18,19]. In this case, the c-axis spinon and holon current-current correlation functions (11) can be evaluated as,

$$\begin{aligned}\Pi_c^{(\mathrm{s})}(\tau-\tau') &= -(t_c e\phi_c)^2 \sum_{l\hat{\eta}_c i i'} [\hat{\eta}_c^2 D_{ab}(l, i-i', \tau-\tau') \\ &\times D_{ab}(l+\hat{\eta}_c, i'-i, \tau'-\tau) \\ &- \hat{\eta}_c^2 D_{ab}(l, i-i', \tau-\tau') D_{ab}(l+\hat{\eta}_c, i'-i, \tau'-\tau) \\ &+ \hat{\eta}_c^2 D_{ab}(l+\hat{\eta}_c, i-i', \tau-\tau') D_{ab}(l, i'-i, \tau'-\tau) \\ &- \hat{\eta}_c^2 D_{ab}(l+\hat{\eta}_c, i-i', \tau-\tau') D_{ab}(l, i'-i, \tau'-\tau) \equiv 0, \end{aligned} \quad (12a)$$

$$\begin{aligned}\Pi_c^{(\mathrm{h})}(\tau-\tau') &= -(2\tilde{t}_c e\chi)^2 \sum_{l\hat{\eta}_c i i'} \hat{\eta}_c^2 g_{ab}(l, i-i', \tau-\tau') \\ &\times g_{ab}(l+\hat{\eta}_c, i'-i, \tau'-\tau). \end{aligned} \quad (12b)$$

Therefore as in the previous discussions [25], we find that there is no the direct contribution to the current-current correlation from spinons, but the strongly correlation between holons and spinons is considered through the spinon's order parameters entering in the holon part of the contribution to the current-current correlation, then the charge dynamics in copper oxide materials is mainly caused by charged holons within the CuO_2 planes, which are strongly renormalized because of the strong interaction with fluctuations of surrounding spinon excitations. In the energy and momentum space, the c-axis holon current-current correlation function (12b) can be expressed as,

$$\begin{aligned}\Pi_c^{(\mathrm{h})}(\mathrm{i}\omega_n) &= -\frac{1}{2}(4\tilde{t}_c e\chi c_0)^2 \frac{1}{N} \\ &\times \sum_k \frac{1}{\beta} \sum_{\mathrm{i}\omega_m'} g_{ab}(k, \mathrm{i}\omega_m' + \mathrm{i}\omega_n) g_{ab}(k, \mathrm{i}\omega_m'), \end{aligned} \quad (13)$$

where $\mathrm{i}\omega_n$ is the Matsubara frequency. Then the c-axis current-current correlation function is essentially determined by the property of the in-plane full holon propagator $g_{ab}(k,\mathrm{i}\omega_n)$, which can be expressed as,

$$\begin{aligned} g_{ab}(k,\mathrm{i}\omega_n) &= \frac{1}{g_{ab}^{(0)-1}(k,\mathrm{i}\omega_n) - \Sigma_{\mathrm{h}}^{(2)}(k,\mathrm{i}\omega_n)} \\ &= \frac{1}{\mathrm{i}\omega_n - \xi_k - \Sigma_{\mathrm{h}}^{(2)}(k,\mathrm{i}\omega_n)}, \end{aligned} \quad (14)$$

where the holon self-energy has been obtained by considering the second-order correction due to the spinon pair bubble as [25],

$$\begin{aligned}\Sigma_{\mathrm{h}}^{(2)}(k,\mathrm{i}\omega_n) &= (Zt)^2 \frac{1}{N^2} \sum_{pp'} (\gamma_{p'-k} + \gamma_{p'+p+k})^2 \frac{B_{p'} B_{p+p'}}{4\omega_{p'}\omega_{p+p'}} \\ &\times \Bigg(2\frac{n_{\mathrm{F}}(\xi_{p+k})[n_{\mathrm{B}}(\omega_{p'}) - n_{\mathrm{B}}(\omega_{p+p'})] - n_{\mathrm{B}}(\omega_{p+p'}) n_{\mathrm{B}}(-\omega_{p'})}{\mathrm{i}\omega_n + \omega_{p+p'} - \omega_{p'} - \xi_{p+k}} \\ &+ \frac{n_{\mathrm{F}}(\xi_{p+k})[n_{\mathrm{B}}(\omega_{p+p'}) - n_{\mathrm{B}}(-\omega_{p'})] + n_{\mathrm{B}}(\omega_{p'}) n_{\mathrm{B}}(\omega_{p+p'})}{\mathrm{i}\omega_n + \omega_{p'} + \omega_{p+p'} - \xi_{p+k}} \\ &- \frac{n_{\mathrm{F}}(\xi_{p+k})[n_{\mathrm{B}}(\omega_{p+p'}) - n_{\mathrm{B}}(-\omega_{p'})] - n_{\mathrm{B}}(-\omega_{p'}) n_{\mathrm{B}}(-\omega_{p+p'})}{\mathrm{i}\omega_n - \omega_{p+p'} - \omega_{p'} - \xi_{p+k}} \Bigg), \end{aligned} \quad (15)$$

with $n_{\mathrm{F}}(\xi_k)$ and $n_{\mathrm{B}}(\omega_k)$ are the Fermi and Bose distribution functions, respectively. For the convenience in the following discussions, the above full holon in-plane Green's function $g_{ab}(k,\mathrm{i}\omega_n)$ also can be expressed as frequency integrals in terms of the spectral representation as,

$$g_{ab}(k,\mathrm{i}\omega_n) = \int_{-\infty}^{\infty} \frac{\mathrm{d}\omega}{2\pi} \frac{A_{\mathrm{h}}(k,\omega)}{\mathrm{i}\omega_n - \omega}, \quad (16)$$

with the in-plane holon spectral function $A_{\mathrm{h}}(k,\omega) = -2\mathrm{Im}\, g_{ab}(k,\omega)$. Then the c-axis optical conductivity in the present theoretical framework is expressed [18] as $\sigma_c(\omega) = -\mathrm{Im}\, \Pi_c^{(\mathrm{h})}(\omega)/\omega$.

3 Charge dynamics for the chain copper oxide materials

We firstly consider the chain copper oxide materials. From the experiments testing the c-axis charge dynamics [10],

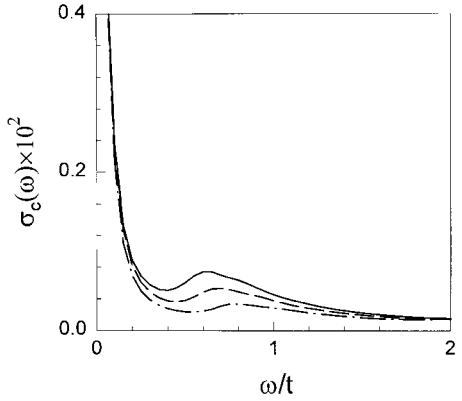

Fig. 1. The *c*-axis optical conductivity σ_c for the chain copper oxide materials at the doping $\delta = 0.12$ (solid line), $\delta = 0.09$ (dashed line), and $\delta = 0.06$ (dot-dashed line) for $t/J = 2.5$, $\tilde{t}_c/t = 0.04$, and $c_0/a_0 = 2.5$ with the temperature $T = 0$.

it has been shown that the presence of the rather conductive Cu-O chains in the underdoped and optimally doped regimes can reduce the blocking effect, and therefore the *c*-axis charge dynamics in this system is effected by the same electron interaction as that in the in-plane. In this case, we substitute equation (16) into equation (13), and evaluate the frequency summations, then the *c*-axis optical conductivity for the chain copper oxide materials can be obtained as [15,18,19],

$$\sigma_c(\omega) = \frac{1}{2}(4\tilde{t}_c e\chi c_0)^2 \frac{1}{N} \times \sum_k \int_{-\infty}^{\infty} \frac{\mathrm{d}\omega'}{2\pi} A_{\rm h}(k,\omega'+\omega) A_{\rm h}(k,\omega') \times \frac{n_{\rm F}(\omega'+\omega) - n_{\rm F}(\omega')}{\omega}, \quad (17)$$

where the in-plane momentum is conserved. This *c*-axis conductivity $\sigma_c(\omega)$ has been calculated numerically, and the result at the doping $\delta = 0.12$ (solid line), $\delta = 0.09$ (dashed line), and $\delta = 0.06$ (dot-dashed line) for the parameters $t/J = 2.5$, $\tilde{t}_c/t = 0.04$, and $c_0/a_0 = 2.5$ at the temperature $T = 0$ is shown in Figure 1, where the charge e has been set as the unit. From Figure 1, we find that there is two bands in $\sigma_c(\omega)$ separated at $\omega \sim 0.4t$, the higher-energy band, corresponding to the "midinfrared band" in the in-plane optical conductivity $\sigma_{ab}(\omega)$ [2,3,25], shows a broad peak at $\omega \sim 0.7t$, in particular, the weight of this band is strongly doping dependent, and decreasing rapidly with dopings, but the peak position does not appreciably shift to higher energies. On the other hand, the transferred weight of the lower-energy band forms a sharp peak at $\omega < 0.4t$, which can be described formally by the non-Drude formula, and our analysis indicates that this peak decay is $\to 1/\omega$ at low energies as in the case of $\sigma_{ab}(\omega)$ [2,3,25]. In comparison with $\sigma_{ab}(\omega)$ [25], the present result also shows that the values of $\sigma_c(\omega)$ are by 2∼3 orders of magnitude smaller than those of $\sigma_{ab}(\omega)$ in the corresponding energy range. The finite temperature behavior of $\sigma_c(\omega)$ also has been discussed, and the result shows that $\sigma_c(\omega)$ is temperature dependent, the higher-energy band is severely suppressed with increasing temperatures, and vanishes at higher temperatures. These results are qualitatively consistent with the experimental results [10] of the chain copper oxide materials and numerical simulations [15].

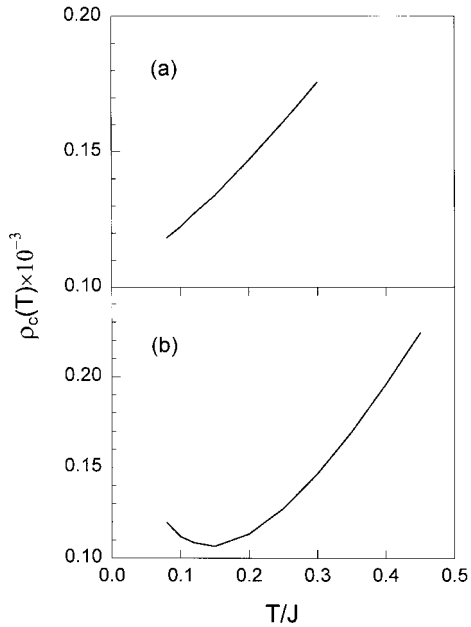

Fig. 2. The *c*-axis electron resistivity ρ_c for the chain copper oxide materials at $t/J = 2.5$, $\tilde{t}_c/t = 0.04$, and $c_0/a_0 = 2.5$ for (a) the doping $\delta = 0.12$ and (b) $\delta = 0.06$.

With the help of the *c*-axis conductivity, the *c*-axis resistivity can be obtained as $\rho_c = 1/\lim_{\omega\to 0}\sigma_c(\omega)$, and the numerical result at the doping $\delta = 0.12$ and $\delta = 0.06$ for the parameters $t/J = 2.5$, $\tilde{t}_c/t = 0.04$, and $c_0/a_0 = 2.5$ is shown in Figures 2a and 2b, respectively. In the underdoped regime, the behavior of the temperature dependence of $\rho_c(T)$ shows a crossover from the high temperature metallic-like ($\mathrm{d}\rho_c(T)/\mathrm{d}T > 0$) to the low temperature semiconducting-like ($\mathrm{d}\rho_c(T)/\mathrm{d}T < 0$), but the metallic-like temperature dependence dominates over a wide temperature range. Therefore in this case, there is a general trend that the chain copper oxide materials show nonmetallic $\rho_c(T)$ in the underdoped regime at low temperatures. While in the optimally doped regime, $\rho_c(T)$ is linear in temperatures, and shows the metallic-like behavior for all temperatures. These results are also qualitatively consistent with the experimental results of the chain copper oxide materials [10] and numerical simulation [15].

4 Charge dynamics for the no-chain copper oxide materials

Now we turn to discuss the *c*-axis charge dynamics of the no-chain copper oxide materials. It has been indicated from the experiments [9] that for the no-chain copper oxide materials the doped holes may introduce a disorder in between the CuO_2 planes, contrary to the case of the chain copper oxide materials [10], where the increasing doping reduces the disorder in between the CuO_2 planes

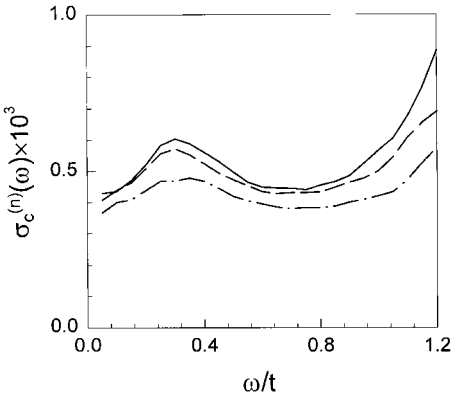

Fig. 3. The c-axis optical conductivity $\sigma_c^{(\mathrm{n})}$ for the no-chain copper oxide materials at the doping $\delta = 0.10$ (solid line), $\delta = 0.08$ (dashed line), and $\delta = 0.06$ (dot-dashed line) for $t/J = 2.5$, $\bar{t}_c/t = 0.04$, and $c_0/a_0 = 2.5$ with the temperature $T = 0$.

due to the effect of the Cu-O chains. Therefore for the no-chain copper oxide materials, the disorder introduced by doped holes residing between the CuO_2 planes modifies the interlayer hopping elements as the random matrix elements. In this case, only the in-plane holon density of states (DOS) $\Omega_{\mathrm{h}}(\omega) = 1/N\sum_k A_{\mathrm{h}}(k,\omega)$ enters the holon current-current correlation function as in disordered systems [15,32], and after a similar discussion as in Section 2, we find that the corresponding momentum-nonconserving expression of the c-axis conductivity $\sigma_c^{(\mathrm{n})}(\omega)$ for the no-chain copper oxide materials is obtained by the replacement of the in-plane holon spectral function $A_{\mathrm{h}}(k,\omega)$ in equation (17) with the in-plane holon DOS $\Omega_h(\omega)$ as [15,32],

$$\sigma_c^{(\mathrm{n})}(\omega) = \frac{1}{2}(4\bar{t}_c e\chi c_0)^2 \int_{-\infty}^{\infty} \frac{\mathrm{d}\omega'}{2\pi} \Omega_{\mathrm{h}}(\omega'+\omega)\Omega_h(\omega') \times \frac{n_{\mathrm{F}}(\omega'+\omega) - n_{\mathrm{F}}(\omega')}{\omega}, \quad (18)$$

where the $\bar{t}_c$ is some average of the random interlayer hopping matrix elements $(\tilde{t}_c)_{li}$. We have performed a numerical calculation for this c-axis conductivity $\sigma_c^{(\mathrm{n})}(\omega)$, and the result at the doping $\delta = 0.10$ (solid line), $\delta = 0.08$ (dashed line), and $\delta = 0.06$ (dash-dotted line) for the parameters $t/J = 2.5$, $\bar{t}_c/t = 0.04$ with the temperature $T = 0$ is plotted in Figure 3. This result shows that the c-axis conductivity $\sigma_c^{(\mathrm{n})}(\omega)$ contains two bands, the higher-energy band, corresponding to the midinfrared band in the in-plane conductivity $\sigma_{ab}(\omega)$ [2,3,25], shows a broad peak at $\sim 0.3t$. The weight of this band is increased with dopings, but the peak position does not appreciably shift to lower energies. As a consequence of this pinning of the transferred spectral weight, the weight of the lower-energy band, corresponding to the non-Drude peak in $\sigma_{ab}(\omega)$ [2,3,25], is quite small and does not form a well-defined peak at low energies in the underdoped and optimally doped regimes. In this case, the conductivity $\sigma_c^{(\mathrm{n})}(\omega)$ at low energies cannot be described by the overdamped Drude-like formula even an ω-dependence of the in-plane holon scattering rate has been taken into consideration. In comparison with the momentum-conserving $\sigma_c(\omega)$, our result also shows that at low energies the suppression of the momentum-nonconserving $\sigma_c^{(\mathrm{n})}(\omega)$ is due to the disordered effect introduced by doped holes residing between the CuO_2 planes. These results are qualitatively consistent with the experimental results of the no-chain copper oxide materials [9].

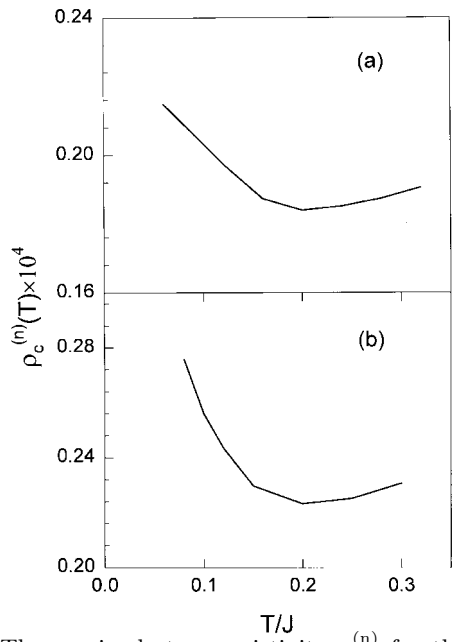

Fig. 4. The c-axis electron resistivity $\rho_c^{(\mathrm{n})}$ for the no-chain copper oxide materials at $t/J = 2.5$, $\bar{t}_c/t = 0.04$, and $c_0/a_0 = 2.5$ for (a) the doping $\delta = 0.10$ and (b) $\delta = 0.06$.

For the further understanding the transport property of the no-chain copper oxide materials, we have also performed the numerical calculation for the c-axis resistivity $\rho_c^{(\mathrm{n})} = 1/\lim_{\omega\to0}\sigma_c^{(\mathrm{n})}(\omega)$, and the results at the doping $\delta = 0.10$ and $\delta = 0.06$ for the parameters $t/J = 2.5$, $\bar{t}_c/t = 0.04$, and $c_0 = 2.5a_0$ are shown in Figures 4a and 4b, respectively. In accordance with the c-axis conductivity $\sigma_c^{(\mathrm{n})}(\omega)$, the behavior of the c-axis resistivity $\rho_c^{(\mathrm{n})}(T)$ in the underdoped and optimally doped regimes is the semiconducting-like at low temperatures, and metallic-like at higher temperatures. In comparison with the in-plane resistivity $\rho_{ab}(T)$ [25], it is shown that the values of the c-axis resistivity $\rho_c^{(\mathrm{n})}(T)$ for the no-chain copper oxide materials are by 3∼4 orders of magnitude larger than these of the in-plane resistivity $\rho_{ab}(T)$ in the corresponding energy range, which are also qualitatively consistent with the experimental results of the no-chain copper oxide materials [9].

5 Summary and discussions

In the above discussions, the central concerns of the c-axis charge dynamics in copper oxide materials are the two dimensionality of the electron state and incoherent hopping between the CuO_2 planes, and therefore the c-axis charge

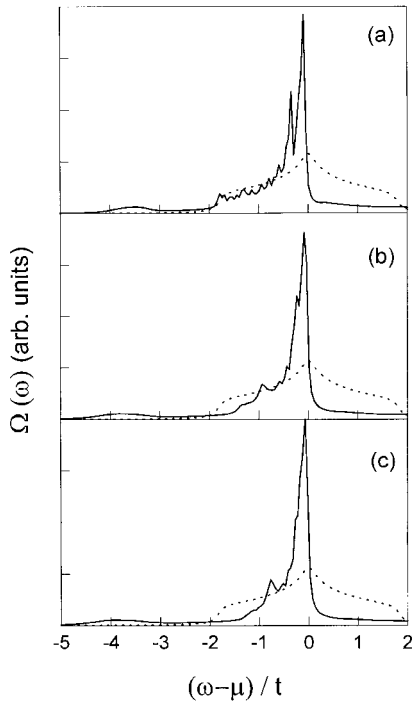

Fig. 5. The in-plane holon density of states at $t/J = 2.5$ for (a) the doping $\delta = 0.06$, (b) $\delta = 0.12$, and (c) $\delta = 0.15$. The dashed line is the result at the mean-field level.

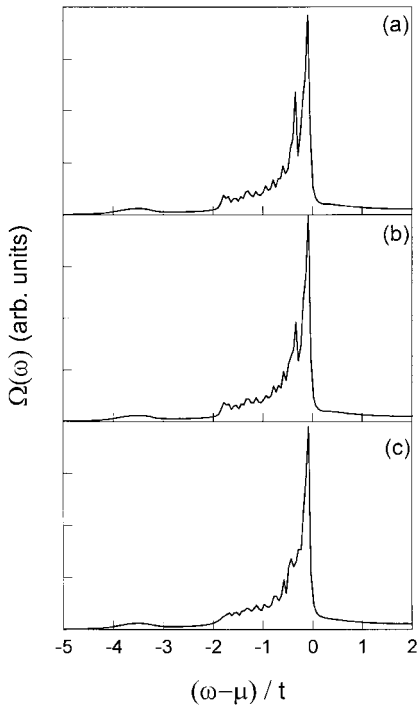

Fig. 6. The in-plane holon density of states for $t/J = 2.5$ at the doping $\delta = 0.06$ for the temperature (a) $T = 0$, (b) $T = 0.01J$, and (c) $T = 0.2J$.

dynamics in the present fermion-spin picture based on the charge-spin separation is mainly determined by the in-plane charged holon fluctuation for the chain copper oxide materials and the in-plane charged holon fluctuation incorporating with the interlayer disorder for the no-chain copper oxide materials. In comparison with the in-plane resistivity $\rho_{ab}(T)$ [25], it is shown that the crossover to the semiconducting-like range in $\rho_c(T)$ is obviously linked with the crossover from the temperature linear to the non-linear range in $\rho_{ab}(T)$, *i.e.*, they should have a common origin.

In the fermion-spin theory [16], the charge and spin degrees of freedom of the physical electron are separated as the holon and spinon, respectively. Although both holons and spinons contributed to the charge and spin dynamics, it has been shown that the scattering of spinons dominates the spin dynamics [31], while the results of the in-plane charge dynamics [25] and present *c*-axis charge dynamics show that scattering of holons dominates the charge dynamics, the two rates observed in the experiments [2] are attributed to the scattering of two distinct excitations, spinons and holons. It has been shown that an remarkable point of the pseudogap is that it appears in both of spinon and holon excitations [1–10]. The present study indicates that the observed crossovers of ρ_{ab} and ρ_c for copper oxide materials seem to be connected with the pseudogap in the in-plane charge holon excitations, which can be understood from the physical property of the in-plane holon DOS. The numerical result of the in-plane holon DOS $\Omega_{\rm h}(\omega)$ at the doping $\delta = 0.06$, $\delta = 0.12$, and $\delta = 0.15$ for the parameter $t/J = 2.5$ at the temperature $T = 0$ is shown in Figures 5a, 5b, and 5c, respectively. For comparison, the corresponding mean-field result (dashed line) is also shown in Figure 5. While the in-plane holon density of states $\Omega_{\rm h}(\omega)$ in the underdoping $\delta = 0.06$ as a function of energy for the temperature (a) $T = 0$, (b) $T = 0.01J$, and (c) $T = 0.2J$ is plotted in Figure 6. From Figures 5 and 6, we therefore find that the in-plane holon DOS in MFA consists of the central part only, which comes from the noninteracting particles as pointed in reference [30]. After including fluctuations the central part is renormalized and two side bands [30] and a V-shape holon pseudogap near the chemical potential μ in the underdoped regime appear. But these two side bands are almost doping and temperature independent, while the V-shape holon pseudogap is doping and temperature dependent, and grows monotonously as the doping δ decreases, and disappear in the overdoped regime. Moreover, this holon pseudogap also decreases with increasing temperatures, and vanishes at higher temperatures. Since the full holon Green's function (then the holon spectral function and DOS) is obtained by considering the second-order correction due to the spinon pair bubble, then the holon pseudogap is closely related to the spinon fluctuation. For small dopings and lower temperatures, the holon kinetic energy is much smaller than the magnetic energy, *i.e.*, $\delta t \ll J$, in this case the magnetic fluctuation is strong enough to lead to the holon pseudogap. This holon pseudogap would reduce the in-plane holon scattering and thus is responsible for the metallic to semiconducting crossover in the *c*-axis resistivity ρ_c and the deviation from the temperature linear behavior in the in-plane resistivity ρ_{ab} [25]. This holon pseudogap will also lead to form the normal-state gap in the system, and the similar result has been

obtained from the doped *kagomé* and triangular antiferromagnets [33], where the strong quantum fluctuation of spinons due to the geometric frustration leads to the normal-state gap. With increasing temperatures or dopings, the holon kinetic energy is increased, while the spinon magnetic energy is decreased. In the region where the holon pseudogap closes, at high temperatures or at higher doping levels, the charged holon scattering would give rise to the temperature linear in-plane resistivity as well as the metallic temperature dependence of the c-axis resistivity. Our results also show that $\rho_{ab}(T)$ is only slightly affected by this holon pseudogap [25], while $\rho_c(T)$ is more sensitive to the underlying mechanism.

In summary, we have studied the c-axis charge dynamics of copper oxide materials in the underdoped and optimally doped regimes within the t-J model by considering the incoherent interlayer hopping. Our result shows the c-axis charge dynamics for the chain copper oxide materials is mainly governed by the scattering from the in-plane fluctuation, and the c-axis charge dynamics for the no-chain copper oxide materials is dominated by the scattering from the in-plane fluctuation incorporating with the interlayer disorder, which would be suppressed when the holon pseudogap opens at low temperatures and lower doping levels, leading to the crossovers to the semiconducting-like range in the c-axis resistivity $\rho_c(T)$ and the temperature linear to the nonlinear range in the in-plane resistivity $\rho_{ab}(T)$. Because copper oxide materials are very complex systems, it is also possible that the actual c-axis conductivity may be a linear combination of the momentum-conserving $\sigma_c(\omega)$ and momentum-nonconserving $\sigma_c^{(\mathrm{n})}(\omega)$, but we believe that $\sigma_c(\omega)$ should be the major part of the c-axis conductivity in the chain copper oxide materials, while $\sigma_c^{(\mathrm{n})}$ should be the major part of the c-axis conductivity in the no-chain copper oxide materials.

The authors would like to thank Professor Ru-Shan Han, Professor H.Q. Lin, Professor T. Xiang, and Professor Z.X. Zhao for helpful discussions. This work was supported by the National Natural Science Foundation under Grant No. 19774014 and the State Education Department of China through the Foundation of Doctoral Training.

References

1. S.L. Cooper, K.E. Gray, in *Physical Properties of High Temperature Superconductors IV*, edited by D.M. Ginsberg (World Scientific, Singapore, 1994), p. 61.
2. See, *e.g.*, *Proceedings of Los Alamos Symposium*, edited by K.S. Bedell *et al.* (Addison-Wesley, Redwood City, California, 1990); A.P. Kampf, Phys. Rep. **249**, 219 (1994).
3. M.A. Kastner *et al.*, Rev. Mod. Phys. **70**, 897 (1998); E. Dagotto, Rev. Mod. Phys. **66**, 763 (1994).
4. P.W. Anderson, *The Theory of Superconductivity in the High-T_c Cuprates* (Princeton, New Jersey, 1997).
5. D.B. Tanner, T. Timusk, in *Physical Properties of High Temperature Superconductors* III, edited by D.M. Ginsberg (World Scientific, Singapore, 1992), p. 363.
6. H. Takagi *et al.*, Phys. Rev. Lett. **69**, 2975 (1992); T. Ito, K. Takenaka, S. Uchida, Phys. Rev. Lett. **70**, 3995 (1993); J.P. Falck *et al.*, Phys. Rev. B **48**, 4043 (1993).
7. H.L. Kao *et al.*, Phys. Rev. B **48**, 9925 (1993); K. Takenaka *et al.*, Phys. Rev. B **50**, 6534 (1994).
8. Y. Nakamura, S. Uchida, Phys. Rev. B **47**, 8369 (1993); X.H. Hou *et al.*, Phys. Rev. B **50**, 496 (1994).
9. S. Uchida, K. Tamasaku, S. Tajima, Phys. Rev. B **53**, 14588 (1996); S. Uchida, Physica C **282-287**, 12 (1997); K. Tamasaku *et al.*, Phys. Rev. Lett. **72**, 3088 (1994);
10. S.L. Cooper *et al.*, Phys. Rev. B **47**, 8233 (1993); S.L. Cooper, *et al.*, Phys. Rev. Lett. **70**, 1533 (1993); J. Schützmann *et al.*, Phys. Rev. Lett. **73**, 174 (1994); A.V. Puchkov *et al.*, Phys. Rev. Lett. **77**, 1853 (1996); C.C. Homes *et al.*, Phys. Rev. Lett. **71**, 1645 (1993);
11. A.J. Leggett, Braz. J. Phys. **22**, 129 (1992).
12. N. Kumar, A. M. Jayannavar, Phys. Rev. B **45**, 5001 (1992).
13. A.G. Rojo, K. Levin, Phys. Rev. B **48**, 16861 (1993).
14. D.G. Clarke, S.P. Strong, P.W. Anderson, Phys. Rev. Lett. **74**, 3088 (1995).
15. P. Prelovšek, A. Ramšak, I. Sega, Phys. Rev Lett. **81**, 3745 (1998).
16. Shiping Feng, Z.B. Su, L. Yu, Phys. Rev. B **49**, 2368 (1994); Mod. Phys. Lett. B **7**, 1013 (1993).
17. Shiping Feng, Yun Song, Phys. Rev. B **55**, 642 (1997).
18. G.D. Mahan, *Many-Particle Physics* (Plenum, New York, 1981).
19. R.H. McKenzie, P. Moses, Phys. Rev. Lett. **81**, 4492 (1998); P.A. Mansky, P.M. Chaikin, R.C. Haddon, Phys. Rev. B **50**, 15929 (1994).
20. P.W. Anderson, in *Frontiers and Borderlines in Many Particle Physics*, edited by R.A. Broglia, J.R. Schrieffer (North-Holland, Amsterdam, 1987), p. 1; Science **235**, 1196 (1987).
21. F.C. Zhang, T.M. Rice, Phys. Rev. B **37**, 3759 (1988).
22. T.M. Rice, in *Proceedings of the International Conference on Materials and Mechanisms of Superconductivity and High Temperature Superconductors V*, Beijing, China, 1997, edited by Y.S. He *et al.* [Physica C **282-287**, xix (1997)], and referenes therein.
23. See, *e.g.*, R.M. Hazen, in *Physical Properties of High Temperature Superconductors* II, edited by D.M. Ginsberg (World Scientific, Singapore, 1990), p. 121.
24. C.M. Fowler *et al.*, Phys. Rev. Lett. **68**, 534 (1992); H. Haghighi *et al.*, Phys. Rev. Lett. **67**, 382 (1991).
25. Shiping Feng, Zhongbing Huang, Phys. Lett. A **232**, 293 (1997); Zhongbing Huang, Shiping Feng, Mod. Phys. Lett. B **12**, 735 (1998).
26. E. Mele, Phys. Scr. T **27**, 82 (1988); E. Fradkin, Phys. Rev. Lett. **63**, 322 (1989).
27. Yun Song, Shiping Feng, Benkun Ma, Commun. Theor. Phys. **31**, 199 (1999).
28. W. Stephan, P. Horsch, Phys. Rev. B **42**, 8736 (1990); A. Moreo, E. Dogotto, Phys. Rev. B **42**, 4786 (1990).
29. L.B. Ioffe, A.I. Larkin, Phys. Rev. B **39**, 8988 (1989).
30. Y.M. Li *et al.*, Phys. Rev. B **45**, 5428 (1992).
31. Shiping Feng, Zhongbing Huang, Phys. Rev. B **57**, 10328 (1998); Zhongbing Huang, Shiping Feng, Phys. Lett. A **242**, 94 (1998).
32. N.F. Mott, E.A. Davis, *Electronic processes in non-crystalline materials* (Clarendon Press, 1979).
33. W.Q. Yu, Shiping Feng, Phys. Rev. B **59**, 13546 (1999); Z.H. Dong, Shiping Feng, Commun. Theor. Phys. **31**, 509 (1999).